

Persistent photoconductivity in $\text{YBa}_2\text{Cu}_3\text{O}_{6+x}$ films as a method of photodoping toward metallic and superconducting phases

V. I. Kudinov, I. L. Chaplygin, A. I. Kirilyuk, and N. M. Kreines

P. Kapitza Institute for Physical Problems, Russian Academy of Sciences, GSP-1, ul. Kosygina 2, Moscow 117973, Russia

R. Laiho and E. Lähderanta

Wihuri Physical Laboratory, University of Turku, Turku, Finland

C. Ayache

Centre d'Etudes Nucleaires de Grenoble, 85X, 38041 Grenoble CEDEX, France

(Received 7 July 1992; revised manuscript received 23 November 1992)

Persistent photoconductivity (PPC) and metastable photoinduced superconductivity, recently discovered in semiconducting $\text{YBa}_2\text{Cu}_3\text{O}_{6+x}$, have been investigated over the oxygen content of $0 < x < 1$. Under exposure of semiconducting $\text{YBa}_2\text{Cu}_3\text{O}_{6+x}$ films ($x \approx 0.4$) to visible light their resistance is found to decrease drastically. After interrupting the irradiation the resistance persists at this reduced level provided that the temperature is kept below 270 K. When the illumination dose is increased the semiconductorlike behavior of the films progressively changes to that of a metal and a superconductor. Prolonged irradiation leads to complete loss of resistivity below 5 K and simultaneous growth of a diamagnetic moment in the films, revealing pronounced enhancement of their superconducting properties. A slow relaxation of the PPC state was found only by warming the sample near to room temperature where it could be described by a thermally activated process with an energy barrier of ~ 1 eV. The observed phenomena are attributed to photoexcitation of extra mobile holes into CuO_2 planes, allowing a metastable superconducting phase to be initiated. We also discuss feasible microscopic mechanisms of PPC in oxygen-deficient Y-Ba-Cu-O films. It is suggested that the photoinduced superconductivity may have applications in fabrication of *in situ* optically tunable weak-link devices.

I. INTRODUCTION

It is well known that high-temperature superconductivity (HTSC) arises from doping of parent metal-oxide semiconductor compounds in the immediate vicinity of the semiconductor-to-metal transition. This is generally made either by chemical substitution of elements as in $\text{La}_{2-x}(\text{Ba},\text{Sr})_x\text{CuO}_{4-y}$ (Refs. 1–4) and $(\text{Pr},\text{Nd},\text{Sm})_{2-x}\text{Ce}_x\text{CuO}_{4-y}$ (Ref. 5) or by varying the oxygen content as in $\text{YBa}_2\text{Cu}_3\text{O}_{6+x}$.^{6–16}

Resistive properties of $\text{YBa}_2\text{Cu}_3\text{O}_{6+x}$ can be changed easily over a wide range, from dielectric to metallic, by varying the oxygen concentration within the limits of $0 \leq x \leq 1$.^{3,13} The unit cell of this compound contains CuO_2 double planes, responsible for the superconducting properties, and CuO_x layers with the oxygen concentration being variable [see Fig. 1(a)]. $\text{YBa}_2\text{Cu}_3\text{O}_6$ ($x=0$) is a dielectric antiferromagnet with a tetragonal crystal lattice.^{3,12,13,15} Increase of x , in the CuO_x layers results in an increase of the free-carrier concentration (holes) in the CuO_2 double layers. At $x \approx 0.4$ the properties of the compound change sharply from semiconducting to metallic involving the superconducting transition at low temperatures. Along with further increase of x , the transition temperature grows to $T_C = 92$ K near $x=1$. A schematic phase diagram^{8,12,16} of $\text{YBa}_2\text{Cu}_3\text{O}_{6+x}$ is shown in Fig. 1(b).

In addition to variation of chemical composition, the

conductivity of semiconductors can be influenced by exiting free carriers with light. Consequently, photoconductivity can be regarded as an alternative method of doping semiconductors,^{17–19} although the number of free carriers remains relatively small. However, superconductivity of the HTSC compounds shows up most vividly in the intermediate vicinity of the semiconductor-to-metal transition. Therefore it can be expected that even a small increase of carrier concentration by photodoping will initiate or enhance their superconductivity.

Measurements of transient photoconductivity have been made on dielectric $\text{YBa}_2\text{Cu}_3\text{O}_{6.3}$ monocrystals,^{17–19} $\text{YBa}_2\text{Cu}_3\text{O}_6$ films,^{20,21} and La_2CuO_4 monocrystals.^{22,23} In the Y-Ba-Cu-O samples utilized in Refs. 17, 20, and 21, the decay time of photoconductivity proved to be short (≈ 1 –100 ns) compared with that observed in La_2CuO_4 (≈ 10 s).²² In $\text{YBa}_2\text{Cu}_3\text{O}_{6.3}$ monocrystals exposed to laser pulses, an increase of conductivity by 10–11 orders or magnitude over that in the unexposed state has been reported.^{17–19} It was supposed that the concentration of photoexcited nonequilibrium carriers reached a great value leading to a transient photoinduced superconducting state with life time of 10–50 ns.

Apart from transient photoconductivity, a number of semiconductors exhibit persistent photoconductivity (PPC). In the PPC state, the excess conductivity persists a long time after switching off the light.^{24–29} This phenomenon has been recently discovered in $\text{YBa}_2\text{Cu}_3\text{O}_{6+x}$ films with $x \approx 0.4$.³⁰ Illuminating the

films with visible light at 100 K for several hours, a drop of their resistance, completely persisting with time after turning off the light, was observed.^{30–35} When the exposure dose was increased, a transition from the semiconducting to a metallic state occurred. As evidenced by simultaneous measurements of conductivity and magnet-

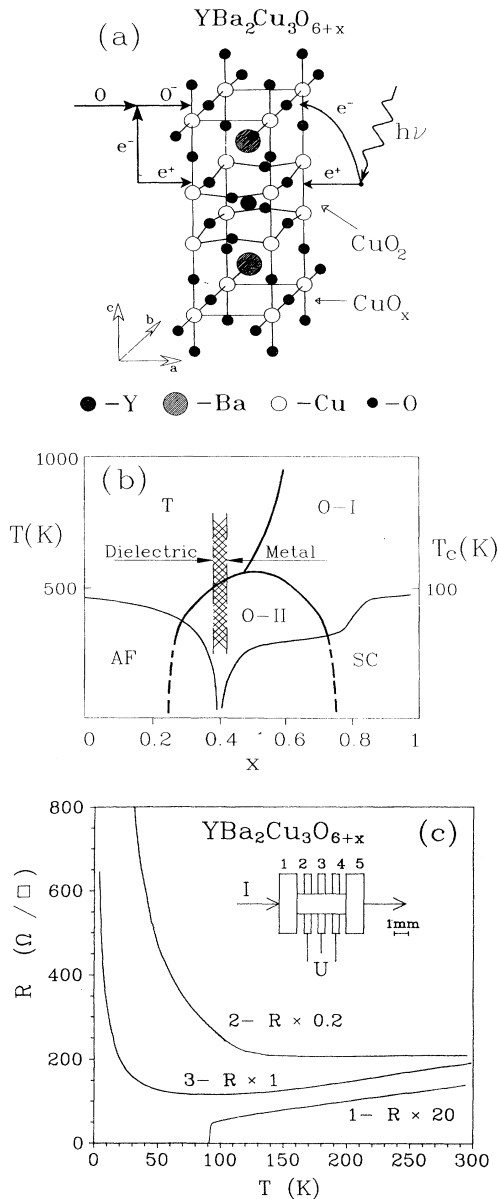


FIG. 1. (a) Crystal structure of $\text{YBa}_2\text{Cu}_3\text{O}_{6+x}$. In the CuO_x layer, the oxygen sites are not fully occupied. The graphs show the charge transfer due to an extra oxygen atom or an absorbed photon. (b) Phase diagram of $\text{YBa}_2\text{Cu}_3\text{O}_{6+x}$, showing the tetragonal (T), orthorhombic ($O-I$ and $O-II$), antiferromagnetic (AF), and superconducting (SC) phases. (c) Temperature dependence of the resistance of $\text{YBa}_2\text{Cu}_3\text{O}_{6+x}$ films with $x=1$ before annealing in vacuum (curve 1), $x=0.35$ (curve 2), and $x=0.38$ (curve 3) after annealing. The inset shows the geometry of the silver contacts on the films.

ic properties of the films irradiated at 5 K, *metastable photoinduced superconductivity* was developed and enhanced with increasing exposure time.^{31,32} The illuminated films showed at room temperature only very slow relaxation of the photoinduced conductivity (relaxation time being of the order of 10 h) toward the equilibrium value. After accomplishing the relaxation at temperatures of 300–320 K, the transport properties of the films were restored to those before illumination. The photoinduced enhancement of superconductivity in $\text{YBa}_2\text{Cu}_3\text{O}_{6+x}$ films has been confirmed in recent experiments.^{36,37}

It was suggested^{31,32} that under illumination of $\text{YBa}_2\text{Cu}_3\text{O}_{6+x}$ films, the concentration of free holes is increased (photodoping), leading to similar effects in transport and magnetic properties as would result from increasing of the oxygen contents of the sample.^{30–37} Early experimental evidence for the PPC and related photoinduced phenomena have been reported in short communications.^{30–35} This paper gives a comprehensive description of extensive investigations into the phenomena of PPC and photoinduced superconductivity, into their relaxation, and dependence on illumination wavelength and on the oxygen concentration. The paper is organized as follows. Sample characteristics and experimental details are presented in Sec. II. Section III contains experimental results of transport and magnetic properties of illuminated films and of the PPC effect. The microscopic mechanism of PPC is discussed in Sec. IV. Conclusions involving possible applications of photoinduced superconductivity are made in Sec. V.

II. SAMPLES

Our samples were prepared from $\text{YBa}_2\text{Cu}_3\text{O}_7$ films grown on SrTiO_3 substrates by laser ablation. The thickness of the films, d , varied from 45 to 90 nm, and their c axis was oriented perpendicular to the surface of the substrate. Silver contacts were deposited on the film surface in the geometry shown in Fig. 1(c). To reduce the oxygen content below the value corresponding to the semiconductor-to-metal transition ($x \approx 0.4$), the films were annealed in vacuum at 320°C for 6–8 h. The oxygen concentration was determined by comparing the lattice parameter c , obtained from x-ray-diffraction measurements, with the data of $c(x)$.⁸ In Ref. 8 oxygen was removed from Y-Ba-Cu-O samples by heating with Zr foil at 415°C, that is, close to the annealing procedure used by us. Compared with untreated $\text{YBa}_2\text{Cu}_3\text{O}_7$ films ($R=6\text{--}20 \Omega/\square$ at 300 K), the resistance of the annealed films was increased by a factor of 10–50. At low temperatures they showed semiconductorlike behavior without any indication of superconductivity.

The resistance measurements were made in an optical Dewar over the temperature range of 2–230 K by using the four-contact dc method. We studied 20 films in all, including the starting material and the following three annealed samples investigated, in detail. Starting material: $x \approx 1$, $d \sim 45\text{--}90$ nm, $R_{300\text{K}}=6\text{--}20 \Omega/\square$, $T_c=89\text{--}91$ K, and transition width ≈ 1 K. Film 1: $x=0.35$, $d \approx 45$ nm, $R_{300\text{K}}=1 \text{ k}\Omega/\square$, $R_{4.2\text{K}}/R_{300\text{K}}$

$=60$, measurements of PPC and $R(T)$. Film 2: $x=0.38$, $d \approx 70$ nm, $R_{300\text{K}} = 200 \Omega/\square$, $R_{4.2\text{K}}/R_{300\text{K}} = 3$, investigation of PPC and relaxation, spectroscopic, transport, and magnetic properties (photoinduced superconductivity). Film 3: $d \sim 90$ nm, study of the dependence of PPC on x .

The oxygen contents of our annealed films suggest that they fall into the semiconducting phase close to the transition from the tetragonal dielectric to the orthorhombic SC phase [see Fig. 1(b)]. This agrees with the temperature dependence of their resistivity, $R(T)$, shown in Fig. 1(c). While the $\text{YBa}_2\text{Cu}_3\text{O}_7$ film (curve 1) reveals a transition to the SC phase below ≈ 90 K, the resistivities of annealed films 1 ($x=0.35$, curve 2) and 2 ($x=0.38$, curve 3) grow monotonically with decreasing temperature. This feature and the large value of $R_{4.2\text{K}}/R_{300\text{K}} = 60$ show that the film 1 is strongly semiconducting. Instead, film 2 is just near the semiconductor-to-metal transition as evidenced by the weak localization regime below 50 K.

The samples were subjected in an optical cryostat to different doses of visible light from Ar, Kr, or HeNe lasers. During illumination, the films were surrounded by gaseous or liquid He in order to avoid diffusion of oxygen out (into) of them. This also prevented overheating of the sample even under the maximum applied photon flux 3×10^{18} photons/(s cm²) (1 W cm^{-2}). The penetration depth of visible light into $\text{YBa}_2\text{Cu}_3\text{O}_{6+x}$ is about 100 nm,³⁸ which is greater than the thicknesses of our films.

III. EXPERIMENTAL RESULTS

A. Transport properties and photoinduced superconductivity

When films 1 and 2 were exposed at 100 K (or 4.2 K) to laser light ($\lambda = 514.5$ nm) for several hours (up to 50 h), their resistances, as shown in Fig. 2, decreased with time (with increasing Q). As the illumination was interrupted at any instant, the lowered value of the resistance remained constant at the preassigned temperature, show-

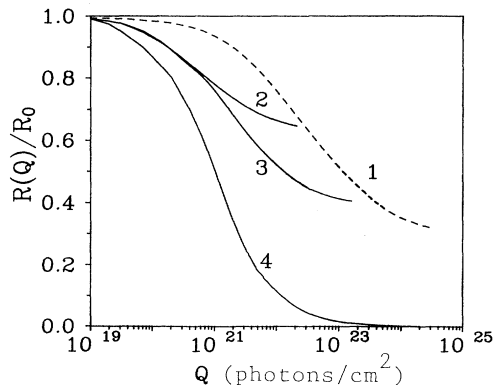


FIG. 2. Resistance of the $\text{YBa}_2\text{Cu}_3\text{O}_{6+x}$ films vs cumulative photon dose Q ($\lambda = 514.5$ nm, flux = 0.2 W/cm^2) of film 1 illuminated at 100 K (curve 1) and film 2 illuminated at 293, 100, and 4.2 K (curves 2–4, respectively).

ing no sign of relaxation below 270 K (the PPC phenomenon).^{30,25,27} After a high illumination does at 100 K, the resistance of the films reached about 40% of the value observed at the same temperature before illumination. Similar results were obtained by irradiating the films with red light from Kr and HeNe lasers.

Illumination by using different laser powers P shows that the PPC effect is a single-valued function of the cumulative photon dose, $Q = P \times t$. This means that we are dealing with a one-photon process, and the effects discussed here can be presented as a function of Q . Upon illumination the resistivity of film 1 changed progressively from “strong” semiconductinglike with $R_{4.2\text{K}}/R_{300\text{K}} = 60$ before illumination (curve 1 in Fig. 3) through a regime with $R_{4.2\text{K}}/R_{300\text{K}} = 14$ (curve 2) to a weak localization regime with $R_{4.2\text{K}}/R_{300\text{K}} = 3$ (curve 3). Between 15 and 60 K, the $R(T)$ curves of film 1 can be approximated by a function $R \propto \exp(E_g/T)$. The semiconducting gap values were found to decrease with increasing photon dose from $E_g = 37$ K before illumination to $E_g = 22$ K after $Q = 1.5 \times 10^{23}$ photons/cm² and $E_g = 12$ K after $Q = 5 \times 10^{23}$ photons/cm². Thus the metallic properties of the film were progressively enhanced. Further illumination of film 1 did not affect substantially its conductivity. At this stage the resistive properties of film 1 ($x=0.35$) became qualitatively similar to those of the unexposed film 2 with oxygen content ($x=0.38$) just near to the semiconductor-to-metal transition.

The resistivity of film 2 can be converted under illumination from a state indicating weak localization behavior to a metallic state with *superconducting properties*. Really, as can be seen from Fig. 4, the semiconductorlike resistivity is suppressed as film 2 is exposed to light (curve 2). In addition, the $R(T)$ curve shows an incident section of resistance below 20 K after $Q = 1.4 \times 10^{22}$ photons/cm² (curve 3). With prolonged exposure the drop of $R(T)$ becomes more pronounced and indicates transitionlike behavior, which moves to higher tempera-

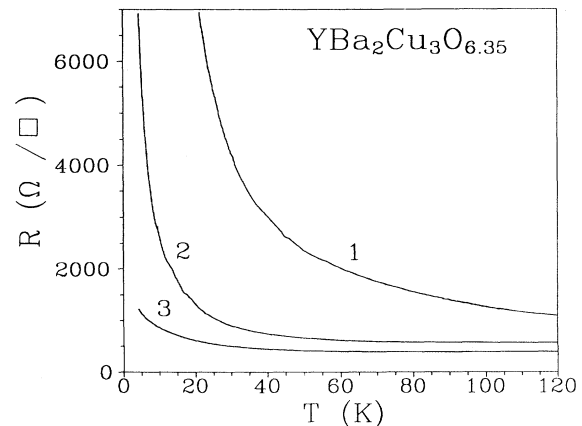


FIG. 3. Temperature dependence of film 1 ($x=0.35$) measured in the dark after illumination at $T = 100$ K ($\lambda = 514.5$ nm) with photon doses $Q=0$ (1), 1.5×10^{23} photons/cm² (2), and 5×10^{23} photons/cm² (3).

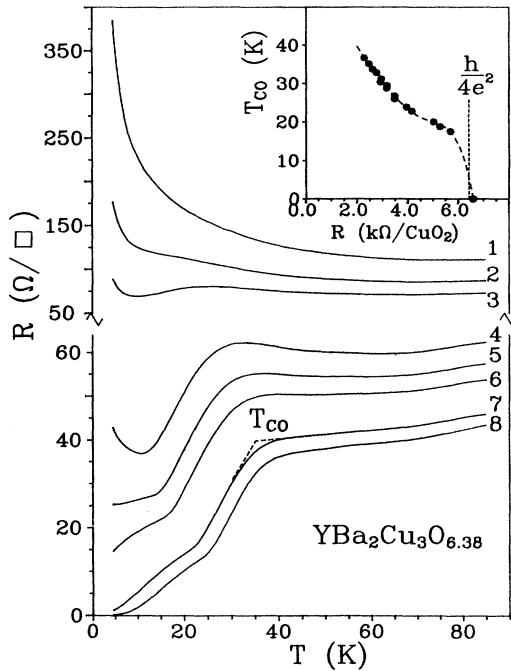


FIG. 4. Temperature dependence of film 2 ($x=0.38$) measured in the dark after illumination at $T=100$ K ($\lambda=514.5$ nm) with photon doses $Q=0$ (1), 4.8×10^{21} photons/cm² (2), 1.4×10^{22} photons/cm² (3), 1.8×10^{22} photons/cm² (4), 3.6×10^{22} photons/cm² (5), 6.3×10^{22} photons/cm² (6), 9.9×10^{22} photons/cm² (7), and 5×10^{23} photons/cm² (8). The inset shows the temperature T_{c0} vs the sheet resistance R (60) calculated for one CuO_x layer at $T=60$ K (normal state).

tures when Q grows. Finally, below 5 K the resistance drops under a measurable level ($R < 0.05 \Omega/\square$) (curve 8). The knee observed in the $R(T)$ curves below 40 K and the strong loss of resistance below it suggest growth of superconducting domains in the sample under illumination. The location of this knee, T_{c0} , is represented in the inset of Fig. 4 as a function of the film resistance calculated at 60 K (normal state) for one CuO_2 layer, R (11.8 Å/ d). The SC state is observed in the illuminated films when the resistance of one double CuO_2 layer is close to $R \approx h/4e^2 = 6.45 \text{ k}\Omega/\square$. This value of R corresponds to the localization threshold of two-dimensional conducting systems.^{39–42} Occurrence of superconductivity close to the localization threshold has been reported also in HTSC compounds^{42–44} where the conductivity was varied by annealing.

The increase of the resistivity at low temperatures (curves 3 and 4 in Fig. 4) and the broad SC transition (curve 8) can be attributed to oxygen inhomogeneity of the film, resulting in properties similar to granular superconductors. Nevertheless, the knee at T_{c0} indicates developing of local superconductivity at intermediate illumination doses. Global superconductivity occurs only at the maximum dose (curve 8) when the resistance drops to zero below 5 K.

Voltage-current characteristics of film 2 were measured by the four-probe method where 1 and 5 are the current

contacts and 2 and 3 (3 and 4) the potential contacts [see inset of Fig. 1(c)]. Before illumination, the V_{23} voltage is a linear function of the I_{15} current. After prolonged illumination ($Q > 5 \times 10^{23}$ photons/cm²), when the film resistance drops to zero below 5 K, its voltage-current characteristic becomes substantially nonlinear like in a system of Josephson-linked superconducting domains (Fig. 5). The critical current of the photoinduced SC phase is about 100 A/cm².

In the transport experiments described above, film 2 was exposed to light at 100 K and the photoinduced superconductivity was observed upon cooling the sample to a low temperature. The photoinduced SC phase could be grown also *in situ* from the semiconducting state at $T < 5$ K. As film 2 was illuminated at 4.2 K (when the SC phase can grow in the film), its resistivity dropped rapidly with time and finally at $Q = 10^{24}$ photons/cm² became at least four to five orders of magnitude lower (see Fig. 2), which is less than the limit of the resistance measurement ($R < 0.05 \Omega/\square$). A similar transition is observed in curve 8 of Fig. 4. The persistent photoconductivity effect is observable even in the metallic phase of $\text{YBa}_2\text{Cu}_3\text{O}_{6+x}$ with $x < 0.45$ (see Sec. IV C 3 below). It has been shown in Ref. 36 that the critical temperature of global superconductivity can be increased substantially by laser illumination.

B. Magnetic properties of the photoinduced SC phase and scenario of photoinduced superconductivity

To verify the superconducting nature of the zero-resistance state occurring in the illuminated $\text{YBa}_2\text{Cu}_3\text{O}_{6+x}$ films at $x \approx 0.4$ and to investigate the growth dynamics of the photoinduced SC phase, the diamagnetic moments of the films were measured as a function of Q . For these investigations film 2 was illuminated at 100 K for periods of 2–3 h. After each period the film was cooled in zero field down to 4.3 K and the magnetic moment was measured by a superconducting quantum interference device (SQUID) magnetometer in a field oriented perpendicular to its surface. The strength of the

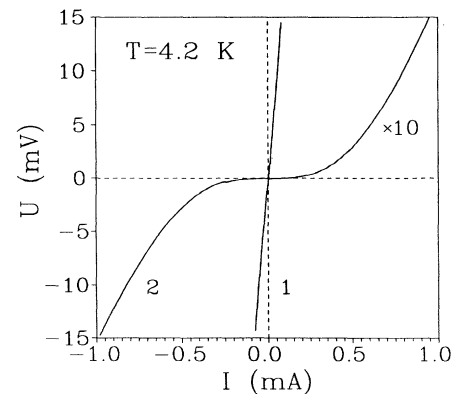


FIG. 5. Voltage-current characteristics of film 2 ($x=0.38$) measured at $T=4.2$ K before (curve 1) and after (curve 2) illumination.

field, 4.5 Oe, corresponded to the middle point of the linear section of the $M(H)$ curve at $T=4.3$ K. In the geometry used, the field practically penetrates into the superconducting domains and the detected diamagnetic moment measures the field screening effect rather than the equilibrium Meissner effect. In this situation the magnitude of the superconducting critical current and vortex-pinning effects dominate the value of the diamagnetic moment.

The results of the magnetic measurements in film 2 are illustrated in Fig. 6(a). The diamagnetic moment does not change practically at low-exposure doses $Q < Q_0 = 6 \times 10^{22}$ photons/cm². However, above this limit the moment starts to grow almost linearly with illumination and comes close to saturation at $Q \approx 2.5 \times 10^{23}$ photons/cm². The total increase of the diamagnetic moment was $\Delta M = -3.3 \times 10^{-8}$ A m². This is about 1% of the moment $M = -4 \times 10^{-6}$ A m² of the original $\text{YBa}_2\text{Cu}_3\text{O}_7$ films measured in the same conditions.

In the above experiments, the transport and magnetic properties of film 2 were measured separately. The obtained results have been confirmed by simultaneous *in situ* measurements of the resistivity and induced diamagnetic moment vs the illumination time for the $\text{YBa}_2\text{Cu}_3\text{O}_{6.4}$ films placed in a SQUID magnetometer.³² When the resistivity of the film dropped as a result of illumination, its diamagnetic moment was found to grow by $\Delta M = -1.2 \times 10^{-8}$ A m².

On basis of the transport and magnetic measurements, the following scenario of the growth of the SC phase in illuminated film 2 can be presented. At low-exposure doses $Q < Q_0 = 6 \times 10^{22}$ photons/cm², the low-temperature conductivity changes gradually from semiconductorlike (curve 1, Fig. 4) to metalliclike (curve 3, Fig. 4) as a result of photogeneration of extra mobile holes. At this stage no SC domains are originated in the film and no increase of the diamagnetic moment is observed [Fig. 6(a)]. At the exposure dose $Q \approx Q_0$, the concentration of the free holes in the CuO_2 layers, N , reaches

the critical value of $N_c \approx 10^{22}$ cm⁻³ (Refs. 45 and 46) at which the SC phase is initiated and starts to grow. Since then, a descending section appears in $R(T)$ (Fig. 4) and the diamagnetic moment grows linearly with the illumination dose [Fig. 6(a)]. With further increase of Q , the size of the SC domains rises and so does the temperature T_{c0} (inset in Fig. 4). The growth of the SC phase (as well as of photoconductivity at 100 K) is saturated at $Q \approx 3 \times 10^{23}$ photons/cm². Obviously, this is the percolation threshold and the resistance becomes zero at 5 K. At the same time, the voltage-current characteristic is rendered nonlinear (Fig. 5).

In principle, an alternative scenario for the superconductivity of the illuminated films can also be presented.⁴⁷⁻⁴⁹ At $x \approx 0.4$ there always exists some oxygen inhomogeneity in the $\text{YBa}_2\text{Cu}_3\text{O}_{6+x}$ films along the sample. Therefore, in the immediate vicinity of the semiconductor-to-metal transition, the films can contain small inclusions of the SC phase. Then it may be assumed that the samples with $x > 0.4$ are composed of superconducting grains and, with $x < 0.4$, of semiconductor interlayers. When the temperature is lowered, the superconductivity of the isolated grains may remain latent because of the growth of the resistance in the semiconductor interlayers. Since the PPC effect occurs in the semiconductor phase only, illumination decreases appreciably the resistance of the interlayers (through photoconductivity) and the SC transition is observed in the $R(T)$ curve. Further illumination enhances the SC properties by initiation of weak superconductivity between the grains in the semiconducting interlayers.⁴⁹

According to the first approach, the photogeneration of free carriers occurs throughout the film. The latter approach accepts the initial inhomogeneity (phase separation) of the sample as an essential ingredient, and the enhancement of superconductivity is associated with appearance of superconducting weak-links between the grains. Recently, the PPC effect has been observed in a homogeneous metallic film ($x > 0.4$) with a narrow SC transition and relatively high T_c .³⁶ Thus the latter explanation of PPC seems unlikely.

C. Persistent photoconductivity

1. Wavelength dependence of the PPC effect

The PPC phenomenon has been observed in our films over the whole temperature range from 1.5 K to room temperatures, where under exposure of film 2 to visible light the resistance is reduced by 30–35 % (see Fig. 2). At illumination doses less than 10^{20} photons/cm², the resistance reduction is linear in time (t), but becomes nonlinear at higher doses and saturates at $Q \approx 1-2 \times 10^{22}$ photons/cm².

The spectral dependence of the persistent photoconductivity has been investigated at 293 K by illuminating $\text{YBa}_2\text{Cu}_3\text{O}_{6+x}$ films through a monochromator (bandwidth 4 nm) by using either a tungsten halogen or a xenon lamp as the light source. The light power was less than 0.4 mW/cm². During the measurements, $R(T)$ was continuously recorded as a function of time. After

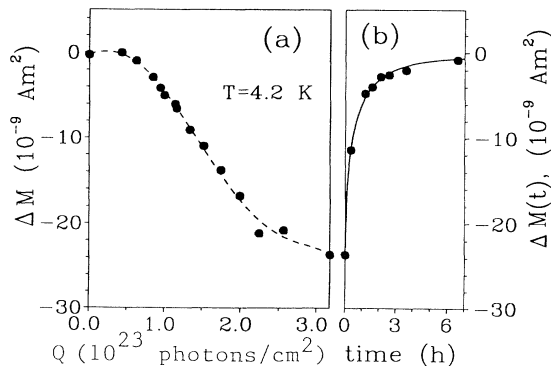


FIG. 6. (a) Photoinduced diamagnetic moment of film 2 vs the illumination dose. (b) Room-temperature relaxation of the diamagnetic moment induced in film 2 by an irradiation dose of 5×10^{23} photon/cm². The solid line is a fit of Eq. (2) to the experimental data.

periods of $\Delta t = 1$ min, the monochromator was turned to the next wavelength using a step of 5 nm. Consequently, the plot of $R(T)$ consisted of segments of straight lines. The spectral efficiency of forming the PPC state in the film at a given light wavelength was determined from the slope of these segments by using the equation

$$\eta(\lambda) = \frac{1}{R(0)} \frac{dR(t)}{dt} \Big|_{t=0} \frac{1}{N_{\text{ph}}(\lambda)}, \quad (1)$$

where $N_{\text{ph}} = P/\hbar\omega$ is the photon-flux density.

The PPC spectrum $\eta(\omega)$ of film 2, as shown in Fig. 7, arises at photon energies above 1.6 eV and has a pronounced maximum at $\hbar\omega = 1.82$ eV. As discussed in detail in our previous publication,³⁵ the spectrum can be presented by a set of six Lorentz lines (dashed lines in Fig. 7) throughout the visible region of 1.6–3.3 eV. The value of the PPC efficiency (quantum efficiency) at its maximum is estimated to be $\eta_{\text{max}} \approx 10^{-4}$ photons⁻¹ for one Cu atom in the CuO₂ layers.

Based on the model of the Mott-Hubbard insulator,^{50–57} the six peaks of the PPC spectra were ascribed to the electronic transitions in the CuO₂ planes, between the conduction band (being formed by five 3d orbitals of Cu²⁺ hybridized with 2p_{x,y} orbitals of O²⁻) and the upper Hubbard unoccupied ($3d_{x^2-y^2}$ Cu²⁺) subband (for details see Ref. 35). In the framework of this model, an interpretation of the structure of the YBa₂Cu₃O_{6+x} conduction band has been given.³⁵ Because the transitions involved have purely electronic origin, it may be expected that $\eta(\omega)$ does not depend strongly on temperature. Upon cooling to low temperatures, the main consequences would be a slight shift of the six Lorentzian peaks to higher energies and some narrowing of their widths.

2. Relaxation of PPC

As noted above, no relaxation of the photoconductivity and induced diamagnetic moment has been found at low

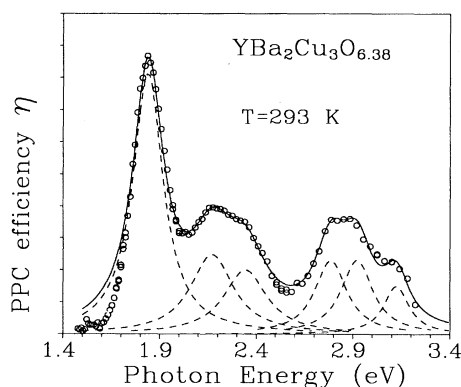


FIG. 7. Spectral efficiency of the growth of PPC, $\eta(\omega)$, in film 2 illuminated at 293 K. The solid line is a fit of $\eta(\omega)$ with six Lorentz peaks, and the dashed lines are contributions of the separate peaks to $\eta(\omega)$.

temperatures. At room temperature, however, a slow relaxation of the conductivity toward the equilibrium value before illumination was observed. The relaxation of the photoinduced excess conductivity of film 2 measured at several temperatures after prolonged illumination (when the PPC effect reached a saturation) is shown in Fig. 8. Obviously, the relaxation time decreases rapidly when the temperature is increased. Besides, the relaxation of PPC is strongly nonexponential. The rate of change is initially rapid, but becomes slower as time progresses. Such behavior is typical to the “stretched-exponential decay,”^{58,59} which in the case of conductivity can be expressed as

$$\Delta\sigma(t) = \Delta\sigma(0) \exp[-(t/\tau)^\beta]. \quad (2)$$

Here τ is a characteristic decay time, β is a dispersion parameter $0 < \beta < 1$, and $\Delta\sigma(t)$ is a deviation of the conductivity from an equilibrium value σ_0 . The stretched-exponential decay has been observed in a wide class of disordered systems such as oxides and polymeric glasses,^{58,59} in spin glasses,^{60–62} and in a charge-density-wave system.⁶³ The Kohlrausch expression (2) has also been used to describe the PPC decay at GaAs interface⁶⁴ and in hydrogenated amorphous silicon.^{65–70}

The solid lines in Fig. 8 show the fits of Eq. (2) to the decay of PPC observed at several temperatures. The values of τ used in the fits are $\tau = 91$ h at $T = 273$ K, $\tau = 4$ h at $T = 293$ K, $\tau = 37.5$ min at $T = 310$ K, and $\tau = 12$ min at $T = 325$ K. The decrease of the relaxation time with increasing temperature can be described by thermally activated relaxation across an energy barrier as

$$\tau(T) = \tau_0 \exp(\Delta/kT), \quad (3)$$

with $\Delta = 0.935$ eV and $\tau_0 = 1.4 \times 10^{-12}$ s (see Fig. 9). The dispersion parameter can be well fitted with a linear function $\beta(T) = -0.63 + T/264.6$ between temperatures of 270 and 330 K.

In the case that the relaxation toward the equilibrium state is statistically independent in each volume element

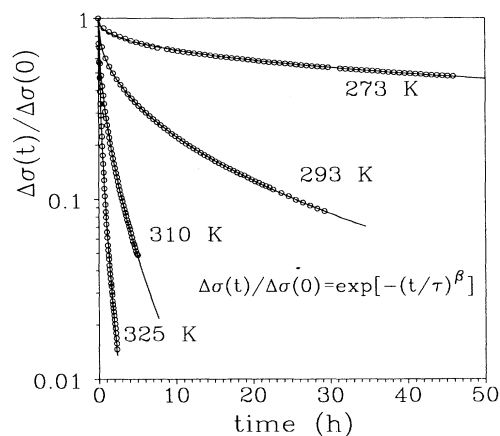


FIG. 8. Relaxation of the photoinduced excess conductivity $\Delta\sigma(t)/\Delta\sigma(0)$ in film 2 at several temperatures. The solid curves are fits of Eq. (2) to the experimental data.

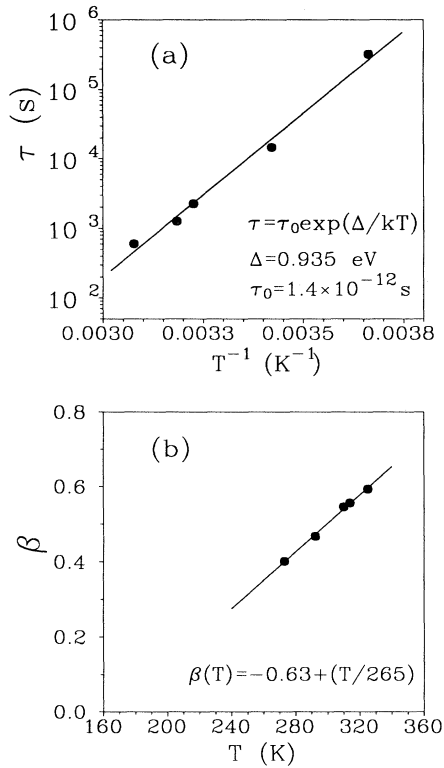


FIG. 9. Temperature dependences of (a) the relaxation time τ and (b) the dispersive parameter β . The solid line (a) is a fit of $\tau(T)$ with Eq. (3) using the values of $\tau_0 = 1.4 \times 10^{-12}$ s and $\Delta = 0.935$ eV. The straight line (b) is calculated from the relation $\beta(T) = -0.63 + T/265$.

of the sample, the conventional Debye relaxation law $\propto \exp(-t/\tau)$ can be applied. Then the characteristic time τ will refer to some averaged decay time, and the quantity $(1-\beta)$ will characterize the width of the trap distribution in our system. In the framework of this approach, the width of the trap distribution in the samples is about $\delta\Delta \sim 0.1$ eV.

TABLE I. Properties of the $\text{YBa}_2\text{Cu}_3\text{O}_{6+x}$ film 3 after each annealing stage: c , lattice parameter; x , oxygen content; σ_0 , conductivity at 273 K; $\Delta\sigma_{\max}$, magnitude of PPC at 273 K; τ_{ill} and β_{ill} , the characteristic time and the dispersive parameter of the growth of PPC at 273 K derived from Eq. (4); and Δ and τ_0 , the relaxation parameters of PPC defined by Eq. (3).

N	c (Å)	x	σ_0 (Ω^{-1})	$\Delta\sigma_{\max}$ (Ω^{-1})	Illumination		Relaxation		
					$\Delta\sigma_m/\sigma_0$ (%)	τ_{ill} (s)	β_{ill}	Δ (eV)	τ_0 (s)
1	11.705	0.9	1.48×10^{-1}	0	0				
2	11.735	0.68	8.34×10^{-2}	0	0				
3	11.752	0.50	6.34×10^{-2}	1.90×10^{-4}	0.3				
4	11.766	0.42	5.75×10^{-2}	2.19×10^{-3}	3.8				
5	11.783	0.405	3.26×10^{-2}	2.82×10^{-3}	8.65	5.34×10^3	0.616	1.290	$\sim 10^{-16}$
6	11.797	0.400	1.64×10^{-2}	3.90×10^{-3}	23.8	9.29×10^3	0.607	1.062	2.3×10^{-14}
7	11.813	0.388	9.78×10^{-3}	5.08×10^{-3}	51.9	2.33×10^4	0.527	0.995	3.2×10^{-13}
8	11.822	0.375	4.89×10^{-3}	4.92×10^{-3}	100.6	2.07×10^4	0.524	0.926	4.8×10^{-12}
9	11.832	0.25	2.23×10^{-3}	1.13×10^{-3}	50.7	1.20×10^4	0.621	0.723	1.7×10^{-8}
10	11.842	0.15	1.25×10^{-3}	4.18×10^{-4}	33.4	1.19×10^5	0.588	0.605	2.6×10^{-6}
11	11.850	0.1	6.12×10^{-4}	0	0				

Figure 6(b) shows the relaxation of the photoinduced diamagnetic moment $\Delta M(t)$ in film 2 after exposure with a dose of $Q \simeq 3.2 \times 10^{23}$ photons/cm². The solid curve is a fit of the data with Eq. (2) by using the parameters $\tau_M = 0.54$ h and $\beta_M = 0.58$. Hence $\Delta M(t)$ decays more rapidly than PPC [$\Delta\sigma(t)$] for which the values of $\tau = 4.06$ h and $\beta = 0.49$ were observed at 293 K.

Room-temperature relaxation of PPC leads to degradation of the photoinduced SC properties of the film at low temperatures. Thus the SC transition observed in the $R(T)$ curve (Fig. 4) disappears gradually as the resistivity relaxes at room (or slightly higher) temperature toward its equilibrium value. As soon as the relaxation is accomplished, the resistivity is restored to that observed before illumination (curve 1 in Fig. 4). Thus the PPC effect and photoinduced superconductivity are, in addition to their stability at low temperatures, completely reversible, allowing the film to be changed by illumination repeatedly from the semiconducting to the superconducting phase and vice versa.

3. Dependence of the PPC effect on the oxygen contents of $\text{YBa}_2\text{Cu}_3\text{O}_{6+x}$ films

Finally, we present results for the dependence of the PPC and its relaxation on the oxygen concentration in $\text{YBa}_2\text{Cu}_3\text{O}_{6+x}$ (film 3) over the range of $0 < x < 1$. The oxygen concentration was reduced in 11 annealing stages (each lasting 1–2 h) in vacuum at 320 °C (see Table I). After each annealing stage, the value of x was determined by measuring $c(x)$ with x-ray diffraction. We estimate that the maximum error in the absolute value of x is $\Delta x \sim 0.1$ and the relative error is $\Delta x \leq 0.01$. The film was illuminated at $T = 273$ K by an Ar-ion laser over long periods (30–40 h) at the power density of 0.5 W/cm² and $\lambda = 514.5$ nm. The time dependence of the resulting growth of the conductivity is shown in Fig. 10 for some intermediate oxygen concentrations.

The PPC effect could be observed in the metallic phase only for $x < 0.45$. The saturation value of PPC at high photon doses increases sharply, attaining a maximum at the metal-to-semiconductor transition when $x \simeq 0.4$.

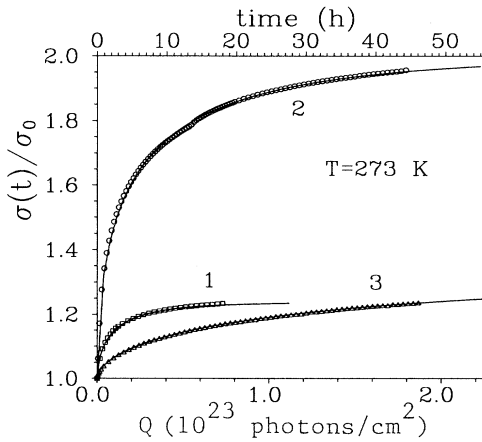


FIG. 10. Normalized conductivity of the $\text{YBa}_2\text{Cu}_3\text{O}_{6+x}$ film 3 vs cumulative photon dose Q at several oxygen contents: $x = 0.40$ (1), $x = 0.375$ (2), and $x = 0.15$ (3). The solid curves are fits of Eq. (4) with the experimental data.

Further oxygen reduction results in a gradual decrease of $\Delta\sigma_{\text{max}}$, and finally the PPC signal disappears at $x \leq 0.1$. Figure 11 illustrates the maximum of the PPC effect, $\Delta\sigma_{\text{max}}$, and its relative value $\Delta\sigma_{\text{max}}/\sigma_0$ vs x , measured at 273 K immediately after prolonged illumination. The semiconductor-to-metal transition can be clearly defined in the equilibrium conductivity $\sigma_0(x)$ measured in the dark.

The relaxation of PPC was measured for each intermediate value of x between $0 < x < 1$. To do this the relaxation curves $\Delta\sigma(x)$ were recorded at $T = 273, 298,$ and 318 K immediately after illumination for 30 min, and the relaxation time τ was determined by fitting the data with Eq. (2) at each temperature involved. For all oxygen concentrations (Fig. 12), τ was found to be very long (several

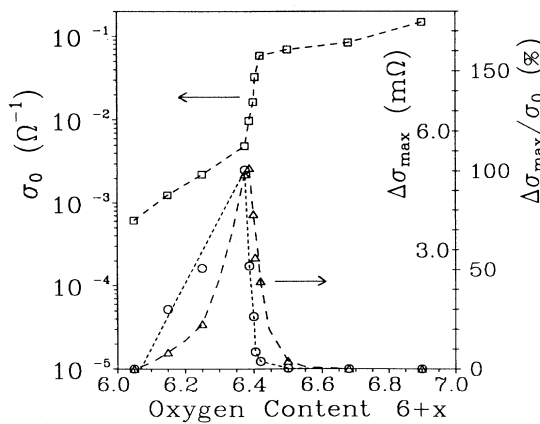


FIG. 11. Magnitude of the PPC effect $\Delta\sigma_{\text{max}}(\Delta)$ and its relative value $\Delta\sigma_{\text{max}}/\sigma_0(\odot)$ vs oxygen concentration of the $\text{YBa}_2\text{Cu}_3\text{O}_{6+x}$ film 3 after prolonged illumination at 273 K and the equilibrium conductivity $\sigma_0(x)$ measured at $T = 273$ K in the dark (\square).

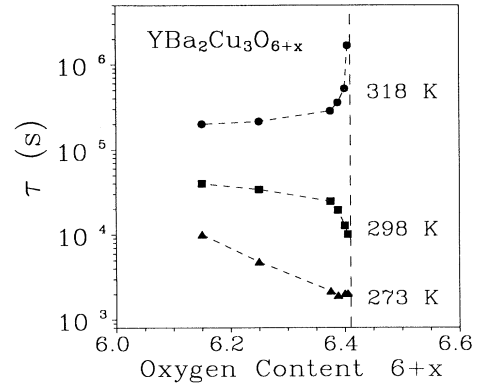


FIG. 12. Decay time of PPC vs oxygen concentration of the $\text{YBa}_2\text{Cu}_3\text{O}_{6+x}$ film 3 at temperatures 273, 298, and 318 K.

hours). The values of $\Delta(x)$ and $\tau_0(x)$ were determined with Eq. (3) by using the data of $\tau(t)$ (see Fig. 9) at each x . As can be seen from Fig. 13, the relaxation barrier Δ increases significantly and τ_0 decreases by orders of magnitude, from 10^{-6} to 10^{-16} s, when the semiconductor-to-metal transition ($x = 0.4$) is approached. The PPC relaxation parameters $\Delta(x)$ and τ_0^{-1} are implicitly correlated with an exponential relationship $\tau_0 = a \exp(-b\Delta)$, where $a = 10^5$ s and $b = 40.5$ eV $^{-1}$. This relationship is well obeyed over a wide range of x except very close to the semiconductor-to-metal transition (see the inset of Fig. 13).

The dependence of the rise of the PPC signal on the illumination time can be expressed in a form similar to Eq. (2),

$$\sigma(t) = \sigma_{\text{max}} - (\sigma_{\text{max}} - \sigma_0) \exp[-(t/\tau_{\text{ill}})^\beta], \quad (4)$$

where σ_{max} is the saturated value of the conductivity and τ_{ill} is a characteristic time of the growth of $\sigma(t)$ (depending on the incident light flux, i.e., $\tau_{\text{ill}} \propto P$). The $\sigma(t)$ curves in Fig. 10 were obtained by fitting Eq. (4) to the observed growth of PPC in film 3 for several oxygen concentrations ($\sigma_{\text{max}}, \tau_{\text{ill}}$, and β_{ill} were used as fitting param-

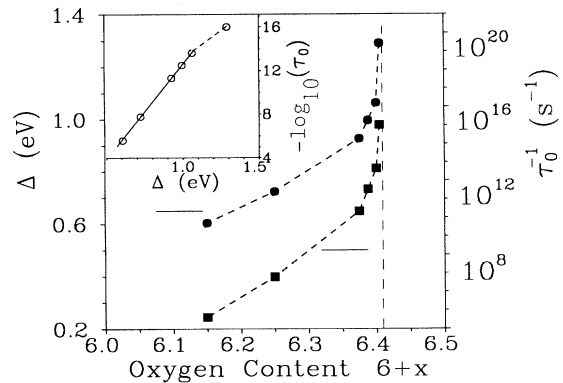


FIG. 13. Dependence of the relaxation parameters Δ and τ_0^{-1} on x in film 3. The inset shows $\ln(\tau_0^{-1})$ plotted vs Δ .

ters). We have observed that $\tau_{\text{ill}}(x)$ increases more than 10 times when x is reduced (see Table I). From these results it may be concluded that the PPC efficiency per one absorbed photon decreases substantially in highly-oxygen-deficient films of $\text{YBa}_2\text{Cu}_3\text{O}_{6+x}$. For $\beta_{\text{ill}}(x)$, a regular trend could not be found in the data.

The barrier of the PPC relaxation remains sufficiently high for all values of x , and the PPC signal does not transform into transient photoconductivity, giving evidence that these two phenomena have different origins in oxygen-deficient $\text{YBa}_2\text{Cu}_3\text{O}_{6+x}$ compounds.

IV. DISCUSSION OF MECHANISMS OF PERSISTENT PHOTOCONDUCTIVITY AND PHOTOINDUCED SUPERCONDUCTIVITY IN $\text{YBa}_2\text{Cu}_3\text{O}_{6+x}$ FILMS

A. Oxygen ordering in $\text{YBa}_2\text{Cu}_3\text{O}_{6+x}$

The semiconductor-to-metal transition in $\text{YBa}_2\text{Cu}_3\text{O}_{6+x}$ is assumed to result from charge transfer from CuO_2 planes to the Cu—O—Cu— chains in the CuO_x layers.^{16,71,72} Accordingly, the p orbitals of O ions in the chains are partially filled and there exist a great number of acceptor centers (localized holes) formed by the unoccupied p orbitals of O^- . At low oxygen content ($x \leq 0.2$), O^{2-} ions turn out to be isolated and each incorporated O ion forms two Cu^{2+} ions.^{9,16,71-74} At $n \geq 2$ ($x > 0.2$), only one oxygen ion appears in a divalent state, O^{2-} , and the other $(n-1)$ oxygen atoms are transformed into the O^- states with simultaneous ionization of $n+1$ Cu^+ ions into a Cu^{2+} state. Thus there are $n-1$ holes in the p orbitals of O ions belonging to a n -mer chain fragment. When x is increased in the CuO_x layers, the concentration of the chain fragments and their average lengths grow. At $x \simeq 0.4$ the average chain length exceeds the critical value ($n_{\text{cr}}=3$ or 4 according to Ref. 72) and it becomes energetically favorable⁷¹⁻⁷⁴ to transfer electrons from CuO_2 planes to the CuO_x layers, inducing thereby hole conductivity in the CuO_2 planes [Fig. 1(a)]. At the same time, the chain fragments are arranged predominantly along the b axis and the tetragonal-to orthorhombic phase transition occurs.

The local oxygen structure in an O-deficient sample depends strongly on the annealing procedure,⁷¹⁻⁷⁸ and a number of metastable phases have been observed.⁷⁹⁻⁸² The oxygen ordering can occur in domains^{73,78} which at low x may be of very small size.^{72,74} On annealing at $T > 500$ K and rapid cooling to room temperature, the metastable disordered O -I phase characterized by a broad distribution of the chain lengths is realized in a sample with $x \sim 0.4$ (or T phase at low x). With increasing x the charge transfer between CuO_x and CuO_2 layers occurs only in the (O -I) domains involving chain fragments with $n > n_{\text{cr}}$ and conducting properties develop in the sample.

A pronounced step in the c lattice parameter at $x=0.4$ (Ref. 8) can be explained by the fact that low-temperature annealing ($T \leq 450^\circ\text{C}$) is favorable for growth of the O -II phase with a narrow distribution of the chain-fragment lengths when compared with the disordered O -I phase.

When approaching the value of $x=0.4$, the charge-transfer process is “switched on” and a relatively narrow semiconductor-to-metal transition occurs. Because our samples were prepared by low-temperature annealing, it is expected that the charge transfer from Cu—O chains to the CuO_2 planes occurs sharply at $x=0.4$. The pronounced maximum of PPC vs x (see Fig. 11) supports this assumption.

Based on the above model of the semiconductor-to-metal transition, we discuss in the following two essentially different mechanisms of PPC in oxygen-deficient $\text{YBa}_2\text{Cu}_3\text{O}_{6+x}$ films. These are the photoinduced charge transfer and the photoinduced diffusion of oxygen.

B. Photoinduced charge-transfer mechanism

Let an absorbed photon excite in an CuO_2 plane an electron into the upper (empty) conduction band. With a certain probability, the electron transfer to an adjacent CuO_x layer where it is trapped in unoccupied p levels of O^- , localized deep in the gap (~ 1.8 eV) between the valence and upper excited bands. The photoexcited holes gradually increase the total concentration of free holes in CuO_2 planes, and the film changes from semiconducting to metallic (*photodoping*). If the concentration of the free carriers corresponds before exposure to the onset of the SC phase ($N \simeq N_c$), photodoping would lead not only to an increase of the conductivity, but also to growth of the SC phase. For $T < 270$ K, the photoexcited electron trapped at O^- is unable to overcome the barrier $\Delta \sim 1$ eV for recombination with a hole. This is why no relaxation of the photoconductivity (and photoinduced superconductivity) is observed in this temperature range. At room temperature the relaxation of PPC is possible by thermal excitation of the trapped electrons over the barrier to the upper conduction band. Inhomogeneity of the oxygen concentration gives rise to some distribution ($\delta\Delta \sim 0.1$ eV) of the trap levels, explaining the reason for the stretched-exponential growth and decay of PPC.

In the framework of the above mechanism, the relaxation parameter $\Delta(x)$ (defined in Sec. II C 2) can be considered as the energy difference between localized O^- levels in the chains and upper conduction band ($d_{x^2-y^2}$ orbitals of Cu^{2+} in CuO_2 planes). Similarly, $\tau_0^{-1}(x)$ is the width of these levels. The energy of the acceptor levels in the chains and their width proved to depend critically on x . At $x \sim 0.1$, O ions are still isolated ($n=1$) and there are no unoccupied O^- levels in the CuO_x layers. In the absence of the acceptor levels at $x \leq 0.15$, the PPC effect was not detected. For $x \geq 0.15$ some chain fragments which can adopt an extra electron appear⁷² and the PPC effect occurs (see Fig. 11). At the same time, the chains lengthen and the acceptor levels are shifted toward the edge of the filled valence band. The O^- level “immersion” corresponds to an increase of the energy barrier, Δ , in Fig. 13. In principle, Δ could rise up to the energy gap of 1.8 eV where the unoccupied levels in the chains can intersect with the filled valence band of CuO_x and the charge-transfer transition occurs. So, owing to increased hybridization between CuO_x and CuO_2 layers, the width of the O^- levels $\propto \tau_0^{-1}$ is increased by orders of magni-

tude up to the value of ~ 1 eV ($\tau_0^{-1} \sim 10^{-16} \text{ s}^{-1}$, Fig. 13). At $x > 0.4$ the transition into the metallic state occurs when the CuO_x and CuO_2 layers become strongly hybridized. Then the photoexcited electrons trapped in the chains are no more isolated from the photogenerated holes in the CuO_2 planes. Under such conditions no quasiequilibrium state can exist and the PPC effect sharply disappears (see Fig. 11).

Although the mechanism discussed above gives an adequate description of many of our experimental results, it is not clear that photoexcited electrons and holes can coexist in a metastable excited state within one unit cell. The orthorhombic structural distortion surrounding a trapped electron^{31,83–85} and the highly anisotropic electronic structure of $\text{YBa}_2\text{Cu}_3\text{O}_{6+x}$ at $x \leq 0.4$ could probably aid in stabilization of the photoexcited electrons.

C. Photoinduced diffusion mechanism

As shown in several works,^{76–78,86} $\text{YBa}_2\text{Cu}_3\text{O}_{6+x}$ has an extraordinarily high diffusivity of oxygen in the CuO_x layers.^{86–88} The activation energy of diffusion depends on the local oxygen structure^{77,78,86–88} and is only 0.11 eV for isolated O ions, while for a jump of an oxygen ion involved in a chain fragment the energy of 1.1–1.3 eV is required (because of the change of the valence). The latter energy corresponds approximately to the barrier of the PPC decay (Fig. 13).

Recently, the relaxation of the metastable tetragonal phase in $\text{YBa}_2\text{Cu}_3\text{O}_{6+x}$ ($x \sim 0.5$) has been studied intensively,^{79–82} showing an increase of T_c by room-temperature aging of oxygen deficient samples quenched from 800 to ~ 300 K. Since no change in the overall oxygen content could be detected, it was suggested that the oxygen rearrangement to the *O*-II phase might be responsible for the effect. Indeed, x-ray diffraction showed an increase of the orthorhombicity during aging. A characteristic time of oxygen reordering, several hours, is similar to the PPC decay time observed by us (see also Ref. 37).

In the tetragonal (semiconducting) phase, O^- ions are randomly arranged among Cu ions so that the probability of finding O^- ions in sites 1 and 2 is the same [Fig. 14(a)]. Suppose that the light absorbed by an oxygen ion in a CuO_x layer transfers the ion to an excited state. The excited ion jumps from position 1 to position 2, where it relaxes and returns to the ground state. In this case two O^- ions may form a chain, originating an orthorhombic ordering of oxygen in CuO_x layers [most likely to the *O*-II phase, Fig. 1(b)]. Above $T \approx 270$ K, the PPC relaxation may be caused by thermal oxygen disordering.

However, there are several experimental results which cannot be satisfactorily explained by the photoinduced diffusion mechanism: (i) The oxygen diffusion presumes rather weak dependence of the relaxation parameters Δ and $\tau_0^{-1} \sim \omega_{\text{ph}}$ on x instead of the observed growth of $\Delta(x)$ and the large increase of $\tau_0(x)$ near $x \approx 0.4$ (Fig. 13). (ii) Assuming that absorbed photons cause jumps of O in the CuO_x layers, the PPC spectrum (Sec. III C 1) should reflect electron transitions in these layers, but not in the CuO_2 planes (Fig. 7).³⁵ (iii) The Hall mobility of

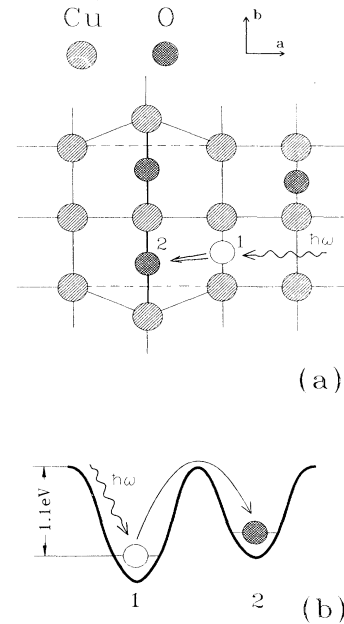


FIG. 14. (a) Photoinduced diffusion of oxygen and forming of a chain fragment and local orthorhombic distortions in CuO_x layers of $\text{YBa}_2\text{Cu}_3\text{O}_{6+x}$ films. (b) Energy diagram of the O atom in the adjacent positions 1 and 2 of CuO_x layers.

quenched nonilluminated $\text{YBa}_2\text{Cu}_3\text{O}_{6+x}$ films reduces during oxygen ordering,³⁷ while the mobility of the sample raises during exposure to light, indicating that the metastable states obtained by photoexcitation and quenching are different.

V. CONCLUSION

We have shown that photoinduced superconductivity and persistent photoconductivity can be generated in a semiconducting $\text{YBa}_2\text{Cu}_3\text{O}_{6.4}$ film by illumination with visible light. In the normal state, the conductivity of the film becomes metallic, as would result from increasing of the oxygen concentration. The illuminated samples exhibit persistent photoconductivity with no sign of relaxation below 270 K and a slow relaxation at 300 K. These processes are completely reversible, allowing the film to be changed repeatedly from semiconducting to superconducting and vice versa.

The metastable state with persistent photoconductivity is probably created by a photoinduced increase of free holes in CuO_2 planes and trapping of electrons on adjacent CuO_x layers. For a selection between this effect and mechanisms such as photoinduced oxygen diffusion, the existence of the localized electron states should be investigated by spectroscopic methods (such as searching for slowly decaying photoluminescence).

Photoinduced superconductivity and persistent photoconductivity offer new possibilities for investigations of the basic mechanisms of $\text{YBa}_2\text{Cu}_3\text{O}_{6+x}$ and other high-temperature superconductors. These phenomena may be

used for designing novel devices by *in situ* laser fabrication⁸⁹ and tuning of superconducting circuits, including SQUID's, with a resolution of the order of 1 μm on a semiconducting $\text{YBa}_2\text{Cu}_3\text{O}_{6.4}$ film. The possibility of varying the local conductivity by illumination in a controlled and reversible manner may find applications in storing and recording of analog and digital information.

ACKNOWLEDGMENTS

The authors gratefully acknowledge A. S. Borovik-Ramanov, J. Flouquet, and G. Uimin for useful discussions. We would like to thank A. Usoskin and I. Chukanova for providing $\text{YBa}_2\text{Cu}_3\text{O}_7$ films and A. Zheludev for assistance in the experiments.

- ¹J. G. Bednorz and K. A. Müller, *Z. Phys.* **64**, 189 (1986).
- ²M. W. Shafer, T. Penney, and B. L. Olson, *Phys. Rev. B* **36**, 4047 (1987).
- ³J. C. Phillips, *Physics of High- T_c Superconductors* (Academic, Orlando, FL, 1989).
- ⁴W. Kang, G. Collin, M. Ribault, J. Friedel, D. Jerome, J. M. Bassat, J. P. Coutures, and Ph. Odiet, *J. Phys. (Paris)* **48**, 1181 (1987).
- ⁵H. Takagi, S. Uchida, and Y. Tokura, *Phys. Rev. Lett.* **62**, 1197 (1989).
- ⁶M. K. Wu, J. R. Ashburn, C. J. Torng, P. H. Hor, R. L. Meng, L. Gao, Z. J. Huang, Y. Q. Wang, and C. W. Chu, *Phys. Rev. Lett.* **58**, 908 (1987).
- ⁷J. D. Jorgensen, M. A. Beno, D. G. Hinks, L. Soderholm, K. J. Volin, R. L. Hitterman, J. D. Grace, I. K. Schuller, C. U. Serge, K. Zhang, and M. S. Kleefisch, *Phys. Rev. B* **36**, 3608 (1987).
- ⁸R. J. Cava, B. Batlogg, K. M. Rabe, E. A. Rietman, P. K. Gallagher, and L. W. Rupp, *Physica C* **156**, 523 (1988).
- ⁹J. D. Jorgensen, B. W. Veal, A. P. Paulikas, L. J. Nowicki, G. W. Crabtree, H. Claus, and W. K. Kwok, *Phys. Rev. B* **41**, 1863 (1990).
- ¹⁰W. R. McKinnon, M. L. Post, L. S. Selwyn, G. Pleizier, J. M. Tarascon, P. Barboux, L. H. Greene, and G. W. Hull, *Phys. Rev. B* **38**, 6543 (1988).
- ¹¹Y. Ueda and K. Kosuge, *Physica C* **156**, 281 (1988).
- ¹²G. Shirane, J. Als-Nielsen, M. Nielsen, J. M. Tranquada, H. Chou, S. Shamoto, and M. Sato, *Phys. Rev. B* **41**, 6547 (1990).
- ¹³J. M. Tranquada, *Earlier and Recent Aspects of Superconductivity*, edited by G. J. Bednorz and K. Müller, Vol. 90 of *Springer Series in Solid State Sciences* (Springer-Verlag, Berlin, 1990), p. 422.
- ¹⁴J. D. Jorgensen and D. G. Hinks, *Neutron News* (Gordon and Breach, New York, 1990).
- ¹⁵J. Rossat-Mignod, L. P. Regnault, J. M. Jurguens, P. Burlet, J. Y. Henry, G. Lapertot, and C. Vettier, in *Dynamics of Magnetic Fluctuations in High T_c Materials*, edited by G. Reiter, P. Horsh, and G. Psaltakis (Plenum, New York, 1990).
- ¹⁶D. de Fontaine, G. Ceder, and M. Asta, *Nature* **343**, 544 (1990).
- ¹⁷G. Yu, A. J. Heeger, G. Stucky, N. Herron, and E. M. McCarron, *Solid State Commun.* **72**, 345 (1989).
- ¹⁸G. Yu, C. H. Lee, A. J. Heeger, N. Herron, and E. C. McCarron, *Phys. Rev. Lett.* **67**, 2581 (1991).
- ¹⁹G. Yu, C. H. Lee, A. J. Heeger, N. Herron, E. C. McCarron, Lig Cong, and A. M. Goldman, *Phys. Rev. B* **45**, 4964 (1992).
- ²⁰R. R. Krichnavak, S. J. Allen, Sui-Wai Chan, F. De Rosa, M. K. Kelly, S. Sampere, C. T. Rogers, and P. F. Miceli, *Proc. Soc. Photo-Opt. Instrum. Eng.* **1187**, 261 (1989).
- ²¹R. Boyn, K. Löbe, H.-U. Habermeier, and N. Pruss, *Physica C* **181**, 75 (1991).
- ²²T. Thio, R. J. Birgeneau, A. Cassanho, and M. A. Kastner, *Phys. Rev. B* **42**, 10 800 (1990).
- ²³G. Yu, C. H. Lee, A. J. Heeger, S.-W. Cheong, and Z. Fisk, *Physica C* **190**, 563 (1992).
- ²⁴A. Rose, *Concepts in Photoconductivity and Allied Problems* (Wiley, New York, 1963).
- ²⁵M. K. Sheinkman and A. Ya. Shik, *Fiz. Tekh. Poluprovodn.* **10**, 209 (1976) [*Sov. Phys. Semicond.* **10**, 128 (1976)].
- ²⁶H. C. Wright, R. J. Downey, and J. R. Canning, *J. Phys. D* **1**, 1593 (1968).
- ²⁷H. J. Queisser, in *Proceedings of the 17th International Conference on the Physics of Semiconductors*, edited by J. D. Chadi, W. A. Harrison (Springer, New York, 1985), p. 1303.
- ²⁸D. E. Theodorou and H. J. Queisser, *Appl. Phys.* **23**, 121 (1980).
- ²⁹H. J. Queisser and D. E. Theodorou, *Phys. Rev. Lett.* **43**, 401 (1979); *Solid State Commun.* **51**, 875 (1984).
- ³⁰A. I. Kirilyuk, N. M. Kreines, and V. I. Kudinov, *Pis'ma Zh. Eksp. Teor. Fiz.* **52**, 696 (1990) [*JETP Lett.* **52**, 49 (1990)].
- ³¹V. I. Kudinov, A. I. Kirilyuk, N. M. Kreines, R. Laiho, and E. Lähderanta, *Phys. Lett. A* **151**, 358 (1990).
- ³²V. I. Kudinov, A. I. Kirilyuk, N. M. Kreines, R. Laiho, and E. Lähderanta, *Phys. Lett. A* **157**, 290 (1991).
- ³³V. I. Kudinov, I. L. Chaplygin, A. I. Kirilyuk, and N. M. Kreines, *Physica C* **185-189**, 1241 (1991).
- ³⁴V. I. Kudinov, I. L. Chaplygin, A. I. Kirilyuk, N. M. Kreines, R. Laiho, and E. Lähderanta, *Physica C* **185-189**, 751 (1991).
- ³⁵C. Ayache, I. L. Chaplygin, A. I. Kirilyuk, N. M. Kreines, and V. I. Kudinov, *Solid State Commun.* **81**, 41 (1992).
- ³⁶G. Niewa, E. Osquiquil, J. Guimpel, M. Maenhoudt, B. Wuyts, Y. Bruynseraede, M. B. Maple, and I. K. Schuller, *Appl. Phys. Lett.* **60**, 2159 (1992).
- ³⁷G. Niewa, E. Osquiquil, J. Guimpel, M. Maenhoudt, B. Wuyts, Y. Bruynseraede, M. B. Maple, and I. K. Schuller, *Phys. Rev. B* **46**, 14 249 (1992).
- ³⁸H. Yasuoka, H. Mazaki, T. Terashima, and Y. Bando, *Physica C* **175**, 192 (1991).
- ³⁹D. B. Haviland, Y. Liu, and A. M. Goldman, *Phys. Rev. Lett.* **62**, 2180 (1989).
- ⁴⁰H. M. Jaeger, D. B. Haviland, B. G. Orr, and A. M. Goldman, *Phys. Rev. B* **40**, 182 (1989).
- ⁴¹A. F. Hebard and M. A. Paalanen, *Phys. Rev. Lett.* **65**, 927 (1990).
- ⁴²T. Wang, K. M. Beauchamp, D. D. Berkley, B. R. Johnson, J.-X. Lui, J. Zhang, and A. M. Goldman, *Phys. Rev. B* **43**, 8623 (1991).
- ⁴³S. Tanda, M. Honma, and T. Nakayama, *Phys. Rev. B* **43**, 8725 (1991).
- ⁴⁴B. Jayaram, P. C. Lanchester, and M. T. Weller, *Phys. Rev. B* **43**, 5444 (1991).
- ⁴⁵N. P. Ong, in *Physical Properties of High-Temperature Superconductors II*, edited by D. M. Ginsberg (World Scientific, Singapore, 1990).
- ⁴⁶A. Levy, J. P. Falck, M. A. Kastner, R. J. Birgeneau, A. T.

- Fiory, A. F. Hebard, W. J. Gallagher, A. W. Kleinsasser, and A. C. Anderson, *Phys. Rev. B* **46**, 520 (1992).
- ⁴⁷I. Giaever, *Phys. Rev. Lett.* **20**, 1286 (1968).
- ⁴⁸G. Deutschor and M. L. Rappaport, *Phys. Lett. A* **71**, 471 (1979).
- ⁴⁹T. Koshindo, S. Takaoka, and K. Murase, *Solid State Commun.* **76**, 31 (1990).
- ⁵⁰N. F. Mott, *Proc. Phys. Soc. London A* **62**, 416, (1949); *Can. J. Phys.* **34**, 1356 (1956).
- ⁵¹J. Hubbard, *Proc. Phys. Soc. London A* **277**, 237 (1964); **281**, 401 (1964).
- ⁵²W. E. Pickett, *Rev. Mod. Phys.* **61**, 433 (1989).
- ⁵³J. Zaanen, G. A. Sawatzky, and J. W. Allen, *Phys. Rev. Lett.* **55**, 418 (1985).
- ⁵⁴V. J. Emery, *Phys. Rev. Lett.* **58**, 2794 (1987).
- ⁵⁵A. Fujimory, E. Takayama-Muromachi, Y. Uchida, and B. Okai, *Phys. Rev. B* **35**, 8814 (1987).
- ⁵⁶J. F. Annett, R. M. Martin, A. K. McMahan, and S. Satpathy, *Phys. Rev. B* **40**, 2620 (1989).
- ⁵⁷L. A. Curtiss and S. W. Tam, *Phys. Rev. B* **41**, 1824 (1990).
- ⁵⁸R. Kohlrusch, *Ann. Phys. (Leipzig)* **12**, 393 (1847).
- ⁵⁹G. Williams and D. C. Watts, *Trans. Faraday Soc.* **66**, 80 (1970).
- ⁶⁰R. V. Chamberlin, G. Mozurkewich, and R. Orbach, *Phys. Rev. Lett.* **52**, 867 (1984).
- ⁶¹K. L. Ngai, A. K. Rajagopal, and C. Y. Huang, *J. Appl. Phys.* **56**, 1714 (1991).
- ⁶²J. M. D. Coey, D. H. Ryan, and R. Buder, *Phys. Rev. Lett.* **58**, 385 (1987).
- ⁶³G. Kriza and G. Mihaly, *Phys. Rev. Lett.* **56**, 2529 (1986).
- ⁶⁴H. J. Queisser, *Phys. Rev. Lett.* **54**, 234 (1985).
- ⁶⁵J. Kakalios, R. A. Street, and W. B. Jackson, *Phys. Rev. Lett.* **59**, 1037 (1987).
- ⁶⁶W. B. Jackson and J. Kakalios, *Phys. Rev. B* **37**, 1020 (1987).
- ⁶⁷A. J. Hamed, *Phys. Rev. B* **44**, 5585 (1991).
- ⁶⁸K. L. Ngai, *Comments Solid State Phys.* **9**, 129 (1979); **9**, 141 (1980).
- ⁶⁹J. M. D. Coey, D. H. Ryan, and R. Buder, *Phys. Rev. Lett.* **58**, 385 (1987).
- ⁷⁰R. G. Palmer, D. L. Stein, E. Abrahams, and P. W. Anderson, *Phys. Rev. Lett.* **53**, 958 (1984).
- ⁷¹B. W. Veal and A. P. Paulikas, *Physica C* **184**, 321 (1991).
- ⁷²G. Uimin, *Mod. Phys. Lett. B* **6**, 2291 (1992).
- ⁷³G. Ceder, M. Acta, and D. de Fontaine, *Physica C* **177**, 106 (1991).
- ⁷⁴H. F. Poulsen, N. H. Andersen, J. V. Andersen, H. Bohr, and O. G. Mouritsen, *Nature* **349**, 594 (1991).
- ⁷⁵S. Pekker, A. Janossy, and A. Rockenbauer, *Physica C* **181**, 11 (1991).
- ⁷⁶H. Claus, S. Yang, A. P. Paulikas, J. W. Downey, and B. W. Veal, *Physica C* **171**, 205 (1990).
- ⁷⁷G. Cannelli, R. Cantelli, F. Cordero, F. Trequattrini, S. Ferraro, and M. Ferretti, *Solid State Commun.* **80**, 715 (1991).
- ⁷⁸G. Cannelli, R. Cantelli, F. Cordero, F. Trequattrini, and M. Ferretti, *Solid State Commun.* **82**, 433 (1992).
- ⁷⁹B. W. Veal, H. You, A. P. Paulikas, H. Shi, Y. Fang, and J. W. Downey, *Phys. Rev. B* **42**, 4770 (1990).
- ⁸⁰J. D. Jorgensen, S. Pei, P. Lightfoot, H. Shi, A. P. Paulikas, and B. W. Veal, *Physica C* **167**, 571 (1990).
- ⁸¹B. W. Veal, A. P. Paulikas, H. You, H. Shi, Y. Fang, and J. W. Downey, *Phys. Rev. B* **42**, 6305 (1990).
- ⁸²G. V. Uimin, V. F. Gantmakher, A. M. Neminsky, L. A. Novomlinsky, D. V. Shovkin, and P. Brill, *Physica C* **192**, 481 (1992).
- ⁸³Y. H. Kim, C. M. Foster, A. J. Heeger, S. Cox, and G. Stucky, *Phys. Rev. B* **38**, 6478 (1988).
- ⁸⁴C. M. Foster, A. J. Heeger, Y. H. Kim, and G. Stucky, *Synth. Met.* **33**, 171 (1989).
- ⁸⁵I. P. Krylov, *Pis'ma Zh. Eksp. Teor. Fiz.* **52**, 1049 (1990) [*JETP Lett.* **52**, 610 (1990)].
- ⁸⁶X. M. Xie, T. G. Chen, and Z. L. Wu, *Phys. Rev. B* **40**, 4549 (1989).
- ⁸⁷D. P. Almond, Q. Wang, J. Freestone, E. F. Lambson, B. Chapman, and G. A. Saunders, *J. Phys. Condens. Matter* **1**, 6853 (1989).
- ⁸⁸S. de Brion, J. Y. Henry, R. Calemczuk, and E. Bonjour, *Europhys. Lett.* **12**, 281 (1990).
- ⁸⁹Y. Q. Shen, T. Freltolf, and P. Vase, *Appl. Phys. Lett.* **59**, 1365 (1991).